

RSC Advances



This is an *Accepted Manuscript*, which has been through the Royal Society of Chemistry peer review process and has been accepted for publication.

Accepted Manuscripts are published online shortly after acceptance, before technical editing, formatting and proof reading. Using this free service, authors can make their results available to the community, in citable form, before we publish the edited article. This *Accepted Manuscript* will be replaced by the edited, formatted and paginated article as soon as this is available.

You can find more information about *Accepted Manuscripts* in the [Information for Authors](#).

Please note that technical editing may introduce minor changes to the text and/or graphics, which may alter content. The journal's standard [Terms & Conditions](#) and the [Ethical guidelines](#) still apply. In no event shall the Royal Society of Chemistry be held responsible for any errors or omissions in this *Accepted Manuscript* or any consequences arising from the use of any information it contains.

Calculations predict a novel desired compound containing eight catenated nitrogen atoms: 1-amino-tetrazolo-[4,5-b]tetrazole

Cite this: DOI: 10.1039/x0xx00000x

Received 00th January 2012,
Accepted 00th January 2012

DOI: 10.1039/x0xx00000x

www.rsc.org/

Piao He^a, Jianguo Zhang^{*a}, Kun Wang^a, Xin Yin^a, Shaowen Zhang^b, Jianshe Jiao^c

^aState Key Laboratory of Explosion Science and Technology, Beijing Institute of Technology, Beijing 100081 P. R. China;

E-mail: zjgbit@bit.edu.cn

^bSchool of Chemistry, Beijing Institute of Technology, Beijing 100081 P. R. China;

^cResearch Institute of FA and ADA Equipment and Technology, General Armament Department, Beijing 100012 P. R. China

A novel 8-N conjoint energetic compound 1-amino-tetrazolo-[4,5-b]tetrazole has been designed and investigated at the DFT-B3LYP/6-311++G** level of theory. The optimized geometry, vibration analysis including thermochemistry and IR spectrum, NMR data, natural bond orbital and charges, HOMO-LUMO orbitals as well as electrostatic potential were calculated for inspecting the electronic structure properties and interactions of chemical bonds. Properties such as density, enthalpy of formation considered the enthalpy of phase transition and detonation performance have been also predicted. As a result, the detonation velocity and pressure of this compound are $8.90\text{km}\cdot\text{s}^{-1}$, 33.83GPa , respectively, As well as the planar double rings (stable) with high-nitrogen structure (energetic), the high positive heat of formation ($792.38\text{kJ}\cdot\text{mol}^{-1}$) and the eminent performance, lead 1-amino-tetrazolo-[4,5-b]tetrazole to maybe a very promising powerful energetic insensitive compound. In addition, the azido-cyclization kinetics of 1-amino-5-azidotetrazole forming the target compound has been investigated. At gaseous case, the reaction barrier is $30.34\text{kcal}\cdot\text{mol}^{-1}$ and the reaction is endothermic as well as non-spontaneous in general conditions. The rate constants are evaluated over a wide temperature region from 200 to 1000K using the transition state theory (TST) and the Arrhenius experience formula has been fitted as well. The theoretical researches on extended nitrogen chains could improve the synthesis of new high-nitrogen materials in the foreseeable future.

Introduction

The development of energetic compounds from the fundamental research to their application is an exciting and challenging area of chemistry. Considering many applications of the energetic compounds as explosives or propellants, it is important to discover new representatives with significant advantages over compounds currently used not only for military but also for civilian purposes. Many new energetic compounds have emerged recently in order to meet the challenging requirements to improve the performance of existing products.

The key requirements include performance, insensitivity, stability, vulnerability, and environmental safety.¹⁻⁵ Over the past decade, energetic heterocyclic compounds have been investigated extensively. Higher energetic performance has always been a primary requirement for research and development of explosives and propellants.⁶ The azido group is often used as a highly energetic ligand in energetic compounds to increase the enthalpy of formation to about $+364\text{kJ}\cdot\text{mol}^{-1}$ along with an increase in nitrogen content.⁷ 5-azidotetrazole with a nitrogen content of 88.28%, was been synthesized in 1939, and many publications have dealt with the synthesis and characterization of these compounds since then.⁸⁻¹⁰

Since 5-azidotetrazoles are very sensitive towards shock and friction, many attempts have been made to desensitize these materials by introduction of aryl and alkyl groups,¹¹ which negatively affects the corresponding detonation performance as well. Tetrazoles offer a good backbone for the development of energetic compounds together with their high thermal stability (due to the aromaticity) and the high heat of formation of +237 kJ·mol⁻¹ (5H-1,2,3,4-tetrazole).¹² Recently, many energetic compounds that contain the tetrazole moiety have been investigated and synthesized.¹³⁻²⁴ Consequently, the isomeric tetrazoles,²⁵ which are formed by an 1,5-dipolar cyclization²⁶ of the polyazides, are potential replacements for the hazardous polyazides.

When the azido group is attached to a C atom adjacent to a nitrogen in a heterocyclic azide, it may spontaneously cyclize to give a tetrazole ring,²⁷ namely, azido-tetrazole chain-ring isomerization, which has been the subject of many studies.²⁸⁻³⁶ In this work, we design a new high-nitrogen compound with double tetrazole rings containing eight catenated nitrogen, which provides high-energy performance. 1-amino-tetrazolo-[4,5-b]tetrazole is first studied detailedly by high-level *ab initio* calculations. We report the electronic structure, thermochemical properties, enthalpy of formation, density, and detonation performance. On the basis of 1-amino-5-azidotetrazole³⁷, its kinetics of azido-cyclization for 1-(amino)-tetrazolo-[4,5-b]tetrazole has been investigated in this paper. The construction of new high-nitrogen structures with highly catenated nitrogen chains³⁸ and the present theoretical study may promote further experimental study on this new energetic material with high performance.

Computational methods

The geometry of 1-amino-tetrazolo-[4,5-b]tetrazole has been optimized using the hybrid DFT-B3LYP method with 6-311++G** basis set. Thermochemical properties and IR spectrum were obtained through harmonic vibrational frequencies at the same level of theory. Meanwhile, natural bond orbital (NBO) charges, the highest occupied molecular orbitals (HOMO) and the lowest unoccupied molecular orbital (LUMO) orbitals as well as electrostatic potential of the title compound were calculated on the B3LYP/6-311++G** level of theory based on the optimized gas-phase structure, while the NMR spectroscopy has been carried out using the 6-311++G (2df, 2pd) basis set for better estimates of chemical shift calculations.

Enthalpy of formation is the most important parameter for energetic compounds. The gas-phase enthalpies of formation at 0 K and 298.15 K were calculated straightforwardly using the atomization energies method.³⁹ Often the standard state of the material of interest corresponds to the condensed phase. Thus, Condensed-phase heats of formation can be determined using the gas-phase enthalpy of formation and enthalpy of phase transition (either sublimation or vaporization) according to Hess' law of constant heat summation⁴⁰:

$$\Delta H(\text{Solid}) = \Delta H(\text{Gas}) - \Delta H(\text{Sublimation}) \quad (1)$$

$$\Delta H(\text{Liquid}) = \Delta H(\text{Gas}) - \Delta H(\text{Vaporization}) \quad (2)$$

Based on the electrostatic potential of a molecule through quantum mechanical prediction, the heat of sublimation either vaporization can be represented as^{41, 42}:

$$\Delta H(\text{Sublimation}) = a(\overline{SA})^2 + b\sqrt{\sigma_{Tot}^2}v + c \quad (3)$$

$$\Delta H(\text{Vaporization}) = a\sqrt{\overline{SA}} + b\sqrt{\sigma_{Tot}^2}v + c \quad (4)$$

Where (*SA*) is the molecular surface area for this structure, σ_{Tot}^2 is described as an indicator of the variability of the electrostatic potential on the molecular surface, and *v* is interpreted as showing

the degree of balance between the positive and negative potentials on the molecular surface. And where *a*, *b*, and *c* are fitting parameters. We further followed the approach of Politzer to predict the heats of sublimation and vaporization of energetic materials then combined these with Eq.1 or Eq.2 to predict solid and liquid enthalpy of formation.

Besides enthalpy of formation, the other critical parameter for energetic material is the crystal packing density, which needs the datum of the molecular volume. The volume was defined as inside a contour of 0.001 electrons/bohr³ density that was evaluated using a Monte Carlo integration. This method has been successfully applied to high-nitrogen compounds.⁴³ 100 single-point calculations were performed for each optimized structure to get an average volume at the B3LYP/6-311++G** level of theory.

The empirical Kamlet-Jacob equations⁴⁴ widely employed to evaluate the energy performance of energetic compounds were used to estimate the detonation velocity and detonation pressure of title compound. Empirical Kamlet-Jacobs equations can be written as follows:

$$D = 1.01 \left(N \overline{M}^{\frac{1}{2}} Q^{\frac{1}{2}} \right)^{\frac{1}{2}} (1 + 1.30\rho) \quad (5)$$

$$P = 1.558\rho^2 N \overline{M}^{\frac{1}{2}} Q^{\frac{1}{2}} \quad (6)$$

Where *D* is the detonation velocity (km/s); *P* is the detonation pressure (GPa); *N* is the moles of detonation gases per gram explosive; \overline{M} is the average molecular weight of these gases; *Q* is the heat of detonation (J/g); and ρ is the loaded density of explosives (g/cm³). In practice, the loading density can only be approximated to a value less than the theoretical density, thus the *D* and *P* values obtained from Eq.5 and Eq.6 can be regarded as their upper limits.

In order to investigate the synthesis feasibility of designed target compound, we studied azido-cyclization kinetics of 1-amino-5-azidotetrazole. The geometries of the relevant stationary points along the reaction pathways were optimized at B3LYP/6-311++G** level of theory. All the stationary points were characterized by their harmonic vibrational frequencies as minima (no imaginary frequency) or saddle points (only one imaginary frequency). The intrinsic reaction coordinate (IRC) was calculated to confirm whether the reaction transition state (TS) is connecting the reactant and product as two minimum points. The thermodynamic energy parameters and potential energy curve were determined from the vibrational frequencies calculated at the same level. Moreover, the rate constants, as well as Arrhenius empirical formula were evaluated over a wide temperature region from 200 to 1000 K based on the traditional transition theory (TST).

All the *ab initio* calculations involved in this work were carried out using the Gaussian 09 program package⁴⁵. The related kinetics of azido-cyclization reaction including rate constant was performed using the VKLab⁴⁶ and POLYRATE 8. 2 program package⁴⁷.

Results and discussion

Molecular Structure

The optimized structure of 1-amino-tetrazolo-[4,5-b]tetrazole (as shown in Fig. 1) corresponds to at least a local energy minimum on the potential energy surface without imaginary frequency at B3LYP / 6-311++G** level of theory. The selected geometry parameters of optimized molecule are listed in Table 1.

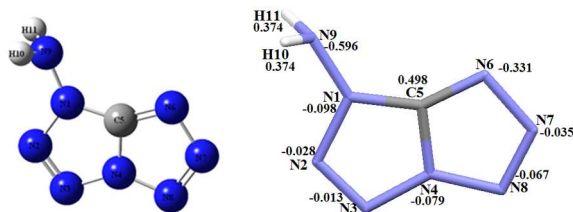


Fig. 1 The optimized geometry and NBO charges (e as unit) of 1-amino-tetrazolo-[4,5-b]tetrazole

It is evident that all N atoms and C atom are in the same plane and 8 N atoms are conjoint directly. And π electrons are delocalized over the ring structure, resulting in such trend of lengths average. The bonding angle of ring atoms is about 108° approximately, which illustrates that the molecule favors five-member ring structure. C and N in the molecule are sp^2 hybridization, forming an approximate planar structure. Such a characteristic is very helpful for the molecular stability. However, there is a certain deviation on angles as a result of the lone pair electrons on N atoms, leading to larger repulsive force when N atoms close to each other. The whole molecule shows stable five-member structure as well as plane double rings without any symmetric properties.

Table 1 Selected parameters of the optimized geometry for 1-amino-tetrazolo-[4,5-b]tetrazole

Bond lengths	Å	Bond angles	(°)	Dihedral angles	(°)
N1-N2	1.377	N1-N2-N3	110.1	N1-N2-N3-N4	-0.07
N2-N3	1.277	N2-N3-N4	105.6	N2-N3-N4-C5	0.05
N3-N4	1.362	N3-N4-C5	112.6	C5-N6-N7-N8	-0.03
N4-C5	1.347	N1-C5-N4	103.0	N9-N1-N2-C5	179.98
C5-N1	1.359	C5-N6-N7	102.9	N2-N1-N9-H10	60.81
C5-N6	1.316	N6-N7-N8	114.3	N2-N1-N9-H11	-60.80
N6-N7	1.372	C5-N1-N9	127.7	C5-N6-N7-N4	-0.01
N7-N8	1.298	N1-N9-H10	109.8	C5-N3-N4-N8	179.98
N8-N4	1.357	N7-N8-N4	103.6		
N9-N1	1.379				

Natural Bond Orbital and charges

Natural Bond Orbital (NBO) charges are considered more reasonable for discussion, exactly what was suggested in Fig.1. The majority of the tetrazole ring's negative charge is localized on the nitrogen atoms in NBO, whereas the positive charge is located on the only carbon atom due to the stronger electronegativity of N element compared with C element. Almost all N atoms display negative charge especially N9 with most negative charge (value of $-0.596e$), which may be because of the inductive effect of $-NH_2$ as electron-withdrawing group. In addition, N6 also displays higher magnitude of the negative charge (value of $-0.331e$) while N1 is distributed less negative charge (value of $-0.098e$) as a result of the same effect. Overall, both positive and negative charges in NBO support the contributing nature of electrons delocalization on tetrazole's ring.

The Wiberg bond index was obtained from NBO calculation. The corresponding results are listed in Table 2, respectively. The Wiberg bond indices of all N-N bonds in the double tetrazoles' ring for title compound are from 1.044 to 1.678 across the overall system. Comparing with these bonds between N1, N2, N3 and N4, the values of bonds between N6, N7, N8 and N4 are little larger from an overall

perspective, which may be attributed to the conjugative effect of right tetrazole-ring. The only C5 atom connected close to N1, N4 and N6 atoms indicates strong covalent characters with each other, promoting the stability of molecular structure.

Table 2 The Wiberg bond index of 1-amino-tetrazolo-[4,5-b]tetrazole

Chemical bonds	Wiberg bond order	Chemical bonds	Wiberg bond order
C5-N4	1.130	N1-N9	1.044
C5-N1	1.120	N9-H10	0.840
C5-N6	1.445	N9-H11	0.840
N2-N1	1.151	N6-N7	1.309
N2-N3	1.678	N7-N8	1.610
N3-N4	1.137	N8-N4	1.147

Frontier molecular orbitals (FMOs)

The highest occupied molecular orbitals (HOMOs) and the lowest unoccupied molecular orbitals (LUMOs) are named as frontier molecular orbitals (FMOs). The HOMO represents the ability to donate an electron, LUMO as an electron acceptor represents the ability to obtain an electron. The energy gap between HOMO and LUMO, which determines the kinetic stability, chemical reactivity and optical polarizability and chemical hardness-softness of a molecule⁴⁸, was calculated at the B3LYP/6-311++G** level⁴⁹.

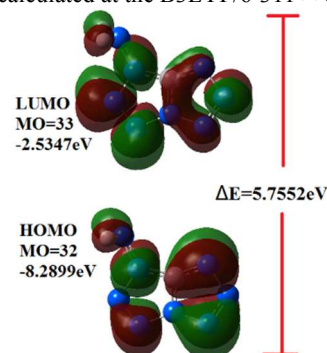


Fig. 2 The HOMO and LUMO orbitals of 1-amino-tetrazolo-[4,5-b]tetrazole

As can be seen in Fig. 2, overlapping of orbital loops located on the HOMO and LUMO, the positive phase is red and the negative one is green. It is clear from the figure that, the HOMO is localized approximately on the right tetrazole ring, while LUMO is localized on the left, which implies that the nitrogen atoms of right tetrazole become the main electron donating group and may be attacked by the electron accepting group. The HOMO→LUMO transition implies an electron density transfer to nitrogen atoms on left tetrazole due to the electrophilic of $-NH_2$. The calculated energy value of HOMO is about -8.2899 eV and LUMO is -2.5347 eV in gaseous phase. The value of energy separation between the HOMO and LUMO is 5.7552 eV.

Electrostatic potential

On the molecular surface, the contribution of electronic and nuclear reach to the extent of counterbalance, while the distribution of the electron density inhomogeneity leads to the molecular surface electrostatic potential is either positive or negative.

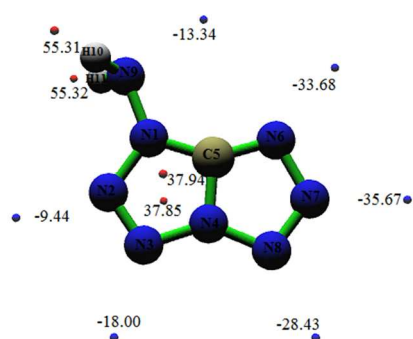
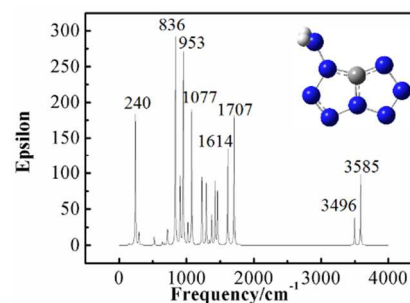
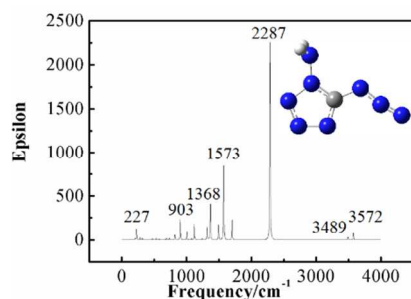


Fig. 3 The electrostatic potential distributions of 1-amino-tetrazolo-[4,5-b]tetrazole

By using the Multiwfn program⁵⁰ based on the Quantitative molecular surface analysis, the extreme value points of electrostatic potential on the molecular surface are visualized in Fig. 3. Firstly, the positive and negative potentials are delocalized inside and outside the rings, respectively. It is evident that there are 6 surface minimum values of negative potential (shown blue points in Fig. 3), which distributes mostly close to nitrogen atoms because of higher electronegativity itself. On the other hand, these positions displayed negative potential, especially near N6 (-33.68 kcal·mol⁻¹), N7 (-35.67 kcal·mol⁻¹) and N8 (-28.43 kcal·mol⁻¹), may react with electrophile such as metal atoms easily. Another 4 surface maximum values of positive potential (shown red points in Fig. 3) prefer to carbon and hydrogen atoms, which illustrates that the electrostatic potential is dominated by nuclear charge. Among them, the electrostatic potential near hydrogen atoms are highest one (55.32 kcal·mol⁻¹) as result of its little electronegativity contrast to carbon and nitrogen atoms. The positions of most positive potential may be attacked easily by the nucleophile to some extent.

Vibration analysis and NMR

All frequency values of molecule are positive, which suggests that they are stable stationary points on the surface of the potential energy. IR spectrum is an effective tool to investigate the basic properties of compounds and identify the substances. Moreover, it is quite related to the thermodynamics properties. The simulated infrared spectra of 1-amino-5-azidotetrazole^[a] and 1-(amino)-tetrazolo-[4,5-b]tetrazole are shown in Fig. 4.



[a] The experimental IR data³⁷ for 1-amino-5-azidotetrazole (cm⁻¹): 3332 (m), 3228 (m), 3162 (w), 2150 (vs), 1635 (m), 1531 (s), 1472 (m), 1404 (w), 1301 (m), 1272 (w), 1191 (m), 1118 (w), 1079 (w), 992 (w), 926 (w), 816(w), 783 (w), 725 (w), 678 (m);

Fig. 4 The IR spectrum of 1-amino-5-azidotetrazole and 1-(amino)-tetrazolo-[4,5-b]tetrazole

The calculated IR results (unscaled) show that 1-amino-5-azidotetrazole compound has two strongest IR peaks at 1573 cm⁻¹ and 2287 cm⁻¹, which are the asymmetrical stretching modes in the ring C-N and N-N of the azido group, respectively. In addition, the amine group was observed vibration modes along with four characteristic peaks in the IR spectrum. The stronger one at 903 cm⁻¹ and 227 cm⁻¹ refer to the N-H bending and out-of-plane deforming and those weaker peaks around 3572 cm⁻¹ and 3489 cm⁻¹ are the asymmetrical and symmetrical stretching of N-H bond on amine group. The fact that the calculated IR data is good agreement with the experiment facilitates us to investigate the title compound. For 1-amino-tetrazolo-[4,5-b]tetrazole, the strongest IR peak at 836 cm⁻¹ corresponds to the N-H symmetrical bending and out-of-plane deforming. While the peak at 1077 cm⁻¹ and 953 cm⁻¹ as medium peaks are mainly dominated by stretching vibration on N-N and C-N of tetrazoles skeleton. The region in 1614 cm⁻¹ is belonging to stretching of tetrazoles as well as the scissor vibration mode of the amine. It is interesting that N-H bonds of the amine have different vibration modes of torsion ranged in 1707 cm⁻¹ and 240 cm⁻¹, and the peak at 3496 and 3585 cm⁻¹ refer to symmetrical asymmetrical stretching vibrations, respectively. It's worth being noticed that the disappearance of peaks at 2287 cm⁻¹ on the azido group and variances on other main peaks predict the azido-tetrazolo tautomerization through comparison with two primary compounds.

On the basis of vibrational analysis and statistic thermodynamic method, thermodynamic functions, such as thermal correction to internal energy (U), enthalpy (H), free energy (G), standard molar heat capacity (C_v) and standard molar thermal entropy (S), as well as zero-point energy (ZPE) of two major compounds are evaluated and tabulated in Table 3. All these values are at 298.25K, 1.00 atm. and with kcal/mol as unit (kca/(mol·K) for S and C_v). All kinds of energy are approximately equal, while the heat capacity and entropy of title compound are smaller than those of 1-amino-5-azidotetrazole, which may confirms the stability of 1-amino-tetrazolo-[4,5-b]tetrazole to some extent.

Table 3 Thermochemical parameters of two major compounds

Species	ZPE	U	H	G	S	C_v
1-Amino-tetrazolo-[4,5-b]tetrazole	42.390	46.441	47.034	22.956	80.756	23.553
1-Amino-5-azidotetrazole	41.802	46.455	47.047	21.409	85.993	25.679

Highly accurate calculations of molecular properties play an important role, especially if they complement experiments that only yield indirect information about molecular and electronic structure as it is the case in NMR spectroscopy. Large, systematic theoretical investigations only allow for reliable error estimates if appropriate experimental studies, such as gas-phase NMR measurements on smaller molecular systems are available.⁵¹ In order to assess the quality of results from DFT methods and the performance of different theoretical basis, calculated shifts of the ¹³C NMR and ¹⁵N NMR for 1-amino-5-azidotetrazole were investigated in details. The chemical shift of only carbon atom on ¹³C NMR was calculated about 158.17ppm, which is good agreement with the experimental shift^[b] (150.60ppm). What holds true in chemical applications – the ¹⁵N NMR spectroscopy often progress stems from the successful interplay between theory and experiment – is also valid for benchmark studies, especially for high-nitrogen compounds. The calculated chemical shifts of all atoms are N3 (27.68), N2 (-0.95), N4 (-66.05), N8 (-142.23), N7 (-154.75), N1 (-167.43), N6 (-320.07) and N9 (-336.99), which are in near quantitative agreement with the experimental values for the ¹⁵N NMR chemical shifts^[b] (0.81, -8.38, -77.26, -141.91, -145.73, -155.13, -300.60, -309.93 ppm). Therefore, the predicted chemical shift for 1-amino-tetrazolo-[4,5-b]tetrazole are 157.15ppm on ¹³C NMR and that of ¹⁵N NMR are 61.91, 8.32, -35.77, -42.98, -72.64, -100.57, -191.27, -334.18ppm, respectively. We included the calculated IR, thermochemical parameters and NMR for easier assignment and positive identification of the target compound.

[b] is the Supporting Information.

Predicted density and detonation performances

To evaluate the utility of new energetic materials, usually their performance characteristics should be calculated. The detonation velocity (V_D) and detonation pressure (P_D) have been evaluated by the empirical Kamlet-Jacobs equations with the above predicted theoretical density and enthalpy of formation in solid phase. Full details of the detonation parameters are listed in Table 4.

Table 4 Detonation Parameters for common HEDMs and two major compounds

Species ^[a]	$\Delta_f H_{298K}(s)$ /kJ·mol ⁻¹	ρ /g·cm ⁻³	v_D /km·s ⁻¹	P_D /GPa
1-amino-tetrazolo- [4,5-b]tetrazole	792.38	1.69	8.90	33.83
1-amino-5- azidotetrazole	721.98	1.62	8.30	28.63
TNT ⁵²	-63.12	1.64	6.95	19.00
RDX ⁵²	79.00	1.80	8.75	34.70
TATB ⁵²	-74.61	1.89	7.86	31.50
FOX-7 ⁵²	-133.7	1.89	8.87	34.00 ^[b]

[a] TNT, trinitrotoluene; RDX, cyclotrimethylene trinitramine; TATB, (2,4,6-trinitro-1,3,5-benzenetriamine); FOX-7, 1,1-diamino-2,2-dinitroethene.

[b] When the experimental data are not available the corresponding data have been calculated using the method in references (as marked with b).

As is evident in Table 4, The title compound 1-amino-tetrazolo-[4,5-b]tetrazole shows a remarkable detonation parameters in comparison with the known compound 1-amino-5-azidotetrazole, which indicates the improvement in high-energy performance. Though the density of this compound is smaller than that of common HEDMs, the detonation velocity (8.90km·s⁻¹) and detonation pressure (33.83GPa) are much greater than those of TNT, RDX and TATB, while almost equals to that of FOX-7 ($V_D=8.87$ km·s⁻¹, $P_D=34.0$ GPa). It is worth noting that 1-amino-tetrazolo-[4,5-b]tetrazole has a perfect character of higher positive enthalpy of formation (792.38kJ·mol⁻¹), which contributes eminent performances. It suggests that this compound might be the promising powerful

energetic materials among the CHNO-containing organic compounds.

Reaction pathways of azido-cyclization

Based on research above, we also investigate the azido-cyclization kinetics of 1-amino-5-azidotetrazole, and Fig. 5 shows the pathways of circulation for 1-amino-tetrazolo-[4,5-b]tetrazole.

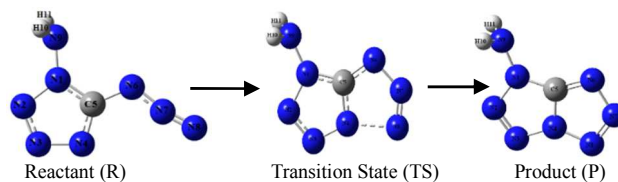


Fig. 5 The synthesis reaction pathways of 1-(amino)-tetrazolo-[4,5-b]tetrazole

All the geometries of stable points along the reaction paths have approximately plane configurations, except for the amine group is lifted out of the ring plane with a dihedral angle of about 69°. Other structural parameters are listed in Table 5. From the reactant, transition state to product 1-amino-tetrazolo-[4,5-b]tetrazole, the most relevant changes upon cyclization concern the bonds N6-N7 and N7-N8, which increase around 0.13 Å and 0.17 Å, while lengths of other bonds on main ring change little to keep relative stable structure. Meanwhile, most bond angles such as N4-C5-N6, C5-N6-N7 and N6-N7-N8 decrease to 110.1°, 102.9° and 114.3°, while N7-N8-N4 increases to 103.6°, which are close to 108° forming a five-member ring. The bond angle C5-N1-N9 of amine reduces around 1° variation compared with the reactant, being unchanged from the overall respective. All the preceding analysis indicates that the obvious ring cyclization occurs mainly in the conversion azido to tetrazole, in which the molecular and electronic structures change significantly.

Table 5 Bond lengths (Å) and angles (°) for the reactant, transition state and product

	N1- N2	N2- N3	N3- N4	N4- C5	C5- N6	C5- N1	N6- N7	N7- N8	N7- N8	N1- N9
R	1.364	1.284	1.363	1.317	1.379	1.351	1.245	1.124	1.385	1.385
TS	1.383	1.278	1.352	1.327	1.349	1.346	1.340	1.194	1.38	1.38
P	1.377	1.277	1.362	1.347	1.316	1.359	1.372	1.298	1.37	1.37
R	N4-C5-N6		C5-N6-N7		N6-N7-N8		N7-N8-N4		C5-N1-N9	
TS	129.2		115.5		171.4		38.9		127.8	
TS	119.0		101.9		127.5		95.3		127.7	
P	110.1		102.9		114.3		103.6		127.7	

To give insight into the electron redistribution in the cyclization, the net charge in the studied compounds was calculated by means of the natural bond orbital (NBO) method. The calculated results were listed in the Table 6. Results indicate that most of the electron redistribution occurs mainly in the azido group and the shift of electrons along the cyclization is highly asynchronous. For example, the net charges of the terminal N8 atom of azido group increase 0.03e for the processes of reactant to TS, while it would decrease about 0.13e for the processes of TS to product. And the difference of net charges residing on the middle N7 atom of azido group, has always decrease about 0.19e and 0.10e for two processes respectively. In addition, the charges on N3 and N4 atoms of tetrazole ring have been found increased to -0.013e and -0.079e as result of electron delocalization. In the whole cyclization process, the electrons transfer rapidly from the tetrazole ring into azido group, which make the two closer nitrogen atoms (the terminal atom

of azido group and the nearest nitrogen atom in the tetrazole ring) possessing the stronger Coulombic interaction.

Table 6 NBO net charges for all atoms along the reaction path (e as unit)

	N1	N2	N3	N4	C5	N6	N7	N8	N9	H10
R	-	-	-	-	+	-	+	+	-	+
	0.095	0.080	0.054	0.352	0.500	0.346	0.256	0.033	0.604	0.371
TS	-	-	-	-	+	-	+	+	-	+
	0.096	0.054	0.015	0.253	0.517	0.376	0.064	0.066	0.598	0.372
P	-	-	-	-	+	-	-	-	-	+
	0.098	0.028	0.013	0.079	0.498	0.331	0.035	0.067	0.596	0.374

Energy parameters and rate constant

The transition state with only one virtual frequency (value of -261.05 cm^{-1}), really connects the reactant and product through the IRC calculation. Fig. 6 depicts the whole reaction potential energy curve.

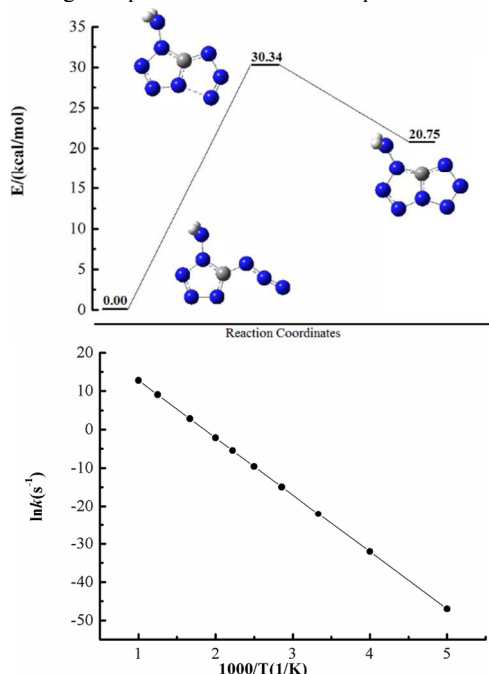


Fig. 6 The potential energy curve and rate constant of azido-cyclization reaction

The energy parameters including the reaction energy ($\Delta_r E$), reaction enthalpy ($\Delta_r H_{298K}^\ominus$) and reaction Gibbs free energy ($\Delta_r G_{298K}^\ominus$), have been obtained by calculating vibration frequency. These results show that the total energy of reaction ($\Delta_r E=20.75 \text{ kcal}\cdot\text{mol}^{-1}$) is positive, means the energy of product is higher. Both reaction enthalpy change ($\Delta_r H_{298K}^\ominus=20.15 \text{ kcal}\cdot\text{mol}^{-1}$) and the Gibbs free energy of reaction ($\Delta_r G_{298K}^\ominus=21.71 \text{ kcal}\cdot\text{mol}^{-1}$) are positive, which imply that the reaction is endothermic and not spontaneous in general conditions. While the calculated theoretical reaction barrier is only $30.34 \text{ kcal}\cdot\text{mol}^{-1}$, indicating that synthesis of 1-amino-tetrazolo-[4,5-b]tetrazole through azido-cyclization of 1-amino-5-azidotetrazole is feasible theoretically. In actual synthesis, some methods such as solvent polarity and electrochemical methods may be used to enhance the reaction conditions, which is conducive to the synthesis of the target compound.

Using the traditional transition state theory, the rate constant of azido-cyclization reaction has been evaluated between 200-1000K temperature regions. Fig.6 displays the reaction rate constant $\ln(k)$ changes linearly with the reciprocal of temperature. As can be seen, the higher temperature makes for accelerating the cyclization

reaction, and when is about 500K the reaction would proceed quickly. In addition, reaction rate constant relationship with the temperature meet the Arrhenius experience formula, the modified equation of three parameters to be corrected and fitted rate constant as follows:

$$k(T) = 9.28 \times 10^{11} \times T^{0.02568} \times e^{-(1.49 \times 10^4/T)} S^{-1}$$

Conclusions

A novel desired compound 1-amino-tetrazolo-[4,5-b]tetrazole containing eight catenated nitrogen atoms has been proposed and investigated by the DFT methods firstly. The optimized geometry, NBO charges, Wiberg bond index, HOMO-LUMO orbital, electrostatic potential, IR spectrum and NMR data as well as thermochemical parameters were calculated for inspecting the electronic structure properties and interactions of chemical bonds with B3LYP/6-311++G** and B3LYP/6-311++G (2df, 2pd) level of theory.

The whole molecule shows stable five-member structure as well as plane double rings without any symmetric properties. Both positive and negative charges in NBO support the contributing nature of electrons delocalization on tetrazole ring. On the other hand, these positions displayed negative electrostatic potential, especially near N6, N7 and N8, may react with electrophile such as metal atoms. The calculated thermochemical parameters, IR and NMR spectrum data has been performed for easier assignment and positive identification of the target compound.

Based on the gas-phase enthalpy of formation derived from atomization energies method, it is more reasonable that the enthalpy of formation in solid were obtained through considering the enthalpy of phase transition. The detonation performance also has been predicted further with theoretical enthalpy of formation and density. It has been confirmed that 1-amino-tetrazolo-[4,5-b]tetrazole might be a very promising energetic (high nitrogen) and insensitive (stable tetrazole double rings) compound with high enthalpy of formation ($792.38 \text{ kJ}\cdot\text{mol}^{-1}$) and exceptional detonation properties ($V_D=8.90 \text{ km}\cdot\text{s}^{-1}$, $P_D=33.83 \text{ GPa}$), equal to the that of FOX-7 to some extent.

In addition, we investigated the azido-cyclization kinetics of 1-amino-5-azidotetrazole forming the target compound. Based on the geometry and NBO charges analysis, indicating that the obvious ring cyclization occurs mainly in the conversion azido to tetrazole, in which the molecular structures and electronic redistribution change significantly. Although, the reaction is endothermic and not spontaneous in general conditions, the reaction barrier of only $30.34 \text{ kcal}\cdot\text{mol}^{-1}$ indicates theoretical feasibility. Finally, the rate constant of azido-cyclization reaction has been evaluated between 200-1000K temperature regions, as well as the Arrhenius experience formula with the modified equation of three parameters, This synthesis of 1-amino-tetrazolo-[4,5-b]tetrazole through azido-cyclization of 1-amino-5-azidotetrazole may be feasible practically when using some methods such as high temperature, solvent polarity and electrochemical methods to enhance the reaction conditions.

Overall, in pursuit of new high-nitrogen structures, a fascinating novel compounds containing eight catenated nitrogen atom chains has been reported firstly, the relative theoretical work of such extended nitrogen chains may open new methods for the synthesis of new high-nitrogen materials in the foreseeable future.

Acknowledgements

The support of the National Natural Science Foundation of China (Grant No. 10776002) and the project of State Key Laboratory of Science and Technology (ZDKT12-03) are gratefully acknowledged.

Notes and references

1. L. Türker and S. Variş, *Polycyclic Aromat. Compd.*, 2009, **29**, 228-266.
2. M. B. Talawar, R. Sivabalan, T. Mukundan, H. Muthurajan, A. K. Sikder, B. R. Gandhe and A. S. Rao, *J. Hazard. Mater.*, 2009, **161**, 589-607.
3. P. K. Swain, H. Singh and S. P. Tewari, *J. Mol. Liq.*, 2010, **151**, 87-96.
4. G. Steinhauser and T. M. Klapötke, *Angew. Chem. Int. Ed.*, 2008, **47**, 3330-3347.
5. T. M. Klapötke and J. Stierstorfer, *Phys. Chem. Chem. Phys.*, 2008, **10**, 4340-4346.
6. H. Gao and J. n. M. Shreeve, *Chem. Rev.*, 2011, **111**, 7377-7436.
7. E. S. Domalski and E. D. Hearing, *J. Phys. Chem. Ref. Data*, 1993, **22**, 805-1159.
8. J. Stierstorfer, T. M. Klapötke, A. Hammerl and R. D. Chapman, *Z. Anorg. Allg. Chem.*, 2008, **634**, 1051-1057.
9. T. M. Klapötke and J. r. Stierstorfer, *J. Am. Chem. Soc.*, 2009, **131**, 1122-1134.
10. A. Hammerl, T. M. Klapötke, P. Mayer, J. J. Weigand and G. Holl, *Propell. Explos. Pyrot.*, 2005, **30**, 17-26.
11. J. C. Kauer and W. A. Sheppard, *J. Org. Chem.*, 1967, **32**, 3580-3592.
12. V. A. Ostrovskii, M. S. Pevzner, T. P. Kofman and I. V. Tselinskii, *Targets Heterocycl. Syst.*, 1999, **3**, 467-526.
13. Z. Liu, Q. Wu, W. Zhu and H. Xiao, *Journal of Physical Organic Chemistry*, 2013, **26**, 939-947.
14. Q.-H. Lin, Y.-C. Li, C. Qi, W. Liu, Y. Wang and S.-P. Pang, *Journal of Materials Chemistry A*, 2013, **1**, 6776.
15. T. M. Klapötke, F. A. Martin and J. Stierstorfer, *Chemistry*, 2012, **18**, 1487-1501.
16. T. M. Klapötke, B. Krumm, F. A. Martin and J. Stierstorfer, *Chemistry, an Asian journal*, 2012, **7**, 214-224.
17. N. Fischer, T. M. Klapötke, M. Reymann and J. Stierstorfer, *Eur. J. Inorg. Chem.*, 2013, **2013**, 2167-2180.
18. D. Fischer, T. M. Klapötke, D. G. Piercey and J. Stierstorfer, *Chemistry*, 2013, **19**, 4602-4613.
19. R. P. Singh, R. D. Verma, D. T. Meshri and J. n. M. Shreeve, *Angew. Chem. Int. Ed.*, 2006, **45**, 3584-3601.
20. M. A. Hiskey, N. Goldman and J. R. Stine, *J. Energ. Mater.*, 1998, **16**, 119-127.
21. S. C. S. Bugalho, E. M. S. Macoas, M. L. S. Cristiano and R. Fausto, *Phys. Chem. Chem. Phys.*, 2001, **3**, 3541-3547.
22. T. Abe, G.-H. Tao, Y.-H. Joo, Y. Huang, B. Twamley and J. n. M. Shreeve, *Angew. Chem. Int. Ed.*, 2008, **47**, 7087-7090.
23. T. M. Klapötke, in *High Energy Density Materials*, Heidelberg, 2007.
24. J. F. Satchell and B. J. Smith, *Phys. Chem. Chem. Phys.*, 2002, **4**, 4314-4318.
25. A. F. Brigas, in *Science of Synthesis*, Stuttgart, 2004.
26. R. Huisgen, *Angew. Chem. Int. Ed. Engl.*, 1968, **7**, 321-328.
27. E. Kessenich, K. Polborn and A. Schulz, *Inorg. Chem.*, 2001, **40**, 1102-1109.
28. T. Lioux, G. Gosselin and C. Mathé, *Eur. J. Org. Chem.*, 2003, **2003**, 3997-4002.
29. M. K. Lakshman, M. K. Singh, D. Parrish, R. Balachandran and B. W. Day, *J. Org. Chem.*, 2010, **75**, 2461-2473.
30. A. Katrusiak, U. Skierska and A. Katrusiak, *J. Mol. Struct.*, 2005, **751**, 65-73.
31. M. Kanyalkar and E. C. Coutinho, *Tetrahedron*, 2000, **56**, 8775-8777.
32. S. L. Deev, Z. O. Shenkarev, T. S. Shestakova, O. N. Chupakhin, V. L. Rusinov and A. S. Arseniev, *J. Org. Chem.*, 2010, **75**, 8487-8497.
33. H. A. Dabbagh and W. Lwowski, *J. Org. Chem.*, 2000, **65**, 7284-7290.
34. I. Alkorta, F. Blanco, J. Elguero and R. M. Claramunt, *Tetrahedron*, 2010, **66**, 2863-2868.
35. I. Alkorta, F. Blanco and J. Elguero, *Tetrahedron*, 2010, **66**, 5071-5081.
36. R. H. Abu-Eittah, F. Taha, M. M. Hamed and K. E. El-Kelany, *J. Mol. Struct. Theochem.*, 2009, **895**, 142-147.
37. T. M. Klapötke, B. Krumm, F. A. Martin and J. Stierstorfer, *Chem. Asian J.*, 2012, **7**, 214-224.
38. Q. Zhang and J. M. Shreeve, *Angew Chem Int Ed Engl*, 2013, **52**, 8792-8794.
39. L. A. Curtiss, K. Raghavachari, P. C. Redfern and J. A. Pople, *J. Chem. Phys.*, 1997, **106**, 1063-1066.
40. P. W. Atkins, *Physical Chemistry*, Oxford University Press, Oxford, 1982.
41. P. Politzer, J. S. Murray, T. Brinck and P. Lane, in *Immunoanalysis of Agrochemicals*, ACS Symp. Ser. 586, American Chemical Society, Washington, DC, 1994.
42. J. S. Murray and P. Politzer, in *Quantitative Treatment of Solute/Solvent Interactions, Theoretical and Computational Chemistry*, Amsterdam, 1994.
43. B. M. Rice, J. J. Hare and E. F. C. Byrd, *J. Phys. Chem. A*, 2007, **111**, 10874-10879.
44. M. J. Kamlet and S. J. Jacobs, *J. Chem. Phys.*, 1968, **48**, 23-35.
45. G. W. S. M.J.T. Frisch, H. B.; Scuseria, G. E.; Robb, M. A.; Cheeseman, J. R.; Montgomery, J. A.; Jr.; Vreven, T.; Kudin, K. N.; Burant, J. C.; Millam, J. M.; Iyengar, S. S.; Tomasi, J.; Barone, V.; Mennucci, B.; Cossi, M.; Scalmani, G.; Rega, N.; Petersson, G. A.; Nakatsuji, H.; Hada, M.; Ehara, M.; Toyota, K.; Fukuda, R.; Hasegawa, J.; Ishida, M.; Nakajima, T.; Honda, Y.; Kitao, O.; Nakai, H.; Klene, M.; Li, X.; Knox, J. E.; Hratchian, H. P.; Cross, J. B.; Bakken, V.; Adamo, C.; Jaramillo, J.; Gomperts, R.; Stratmann, R. E.; Yazyev, O.; Austin, A. J.; Cammi, R.; Pomelli, C.; Ochterski, J. W.; Ayala, P. Y.; Morokuma, K.; Voth, G. A.; Salvador, P.; Dannenberg, J. J.; Zakrzewski, V. G.; Dapprich, S.; Daniels, A. D.; Strain, M. C.; Farkas, O.; Malick, D. K.; Rabuck, A. D.; Raghavachari, K.; Foresman, J. B.; Ortiz, J. V.; Cui, Q.; Baboul, A. G.; Clifford, S.; Cioslowski, J.; Stefanov, B. B.; Liu, G.; Iashenko, A.; Piskorz, P.; Komaromi, I.; Martin, R. L.;

- Fox, D. J.; Keith, T.; Al-Laham, M. A.; Peng, C. Y.; Nanayakkara, A.; Challacombe, M.; Gill, P. M. W.; Johnson, B.; Chen, W.; Wong, M. W.; Gonzalez, C.; Pople, J. A., GAUSSIAN 9 (Revision A.01), Gaussian, Inc, 2009.
46. S. W. Zhang and T. N. Truong, VKLab version1.0 [CP/ CD], Minneapolis: University of Minnesota, Utah: University of Utah, 2001.
47. Y. Y. Chuang, J. C. Corchado and P. L. Fast, POLYRATE, Program vision 8. 2 [CP/CD], Minneapolis: University of Minnesota, 1999.
48. B. Kosar and C. Albayrak, *Spectrochim. Acta, Part A*, 2011, **78**, 160-167.
49. A. Suvitha, S. Periandy, S. Boomadevi and M. Govindarajan, *Spectrochim. Acta, Part A*, 2014, **117**, 216-224.
50. T. Lu, Multiwfn, version 1.4, <http://multiwfn.codeplex.com/>.
51. A. A. Auer, *Chem. Phys. Lett.*, 2009, **467**, 230-232.
52. P. Politzer and J. S. Murray, *Cent. Eur. J. Energ. Mater.*, 2011, **8**, 209-220.